

Figure S1. Lack of Crb2a staining in *crb2a* mutant hearts.

(A-B'') Crb2a immunostaining in 79 hpf Tg(*myI7:ras-EGFP*) *crb2a*^{+/+} (A-A'') and *crb2a*^{-/-} (B-B'') hearts. White arrowheads point to apical localization of Crb2a in *crb2a*^{+/+} compact layer CMs (A''), while ∅ indicates lack of Crb2a immunostaining in *crb2a*^{-/-} hearts (B''). V, ventricle. Scale bars, 20 μm.

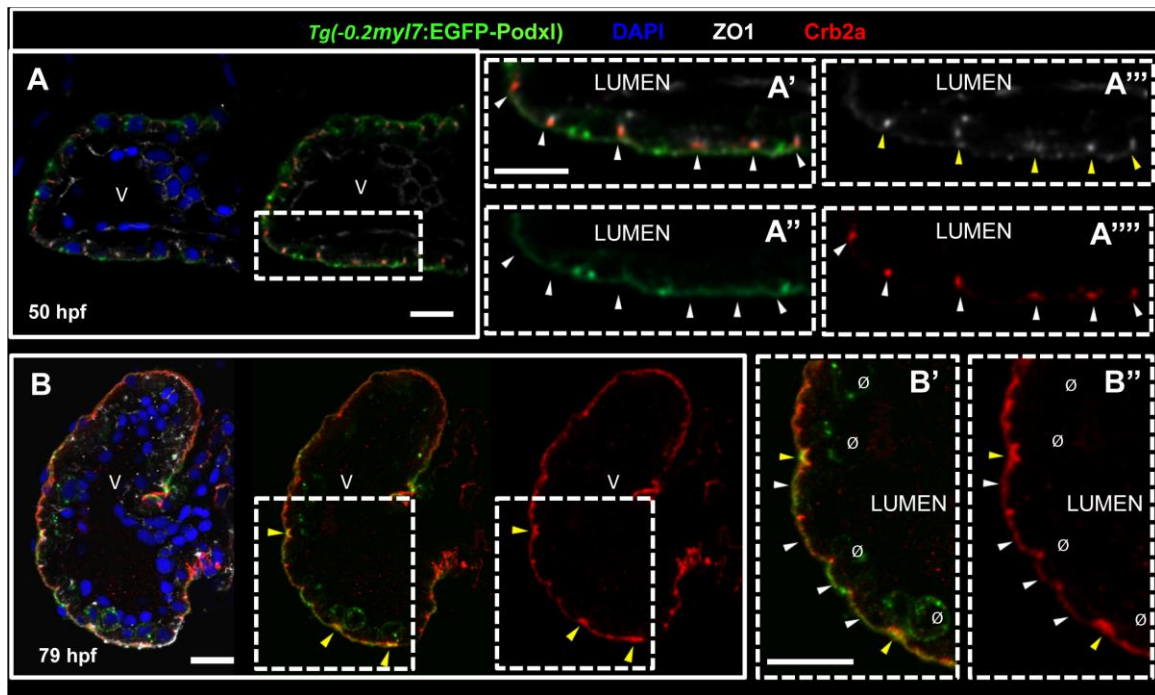


Figure S2. Crb2a co-localizes with ZO-1 in early CMs and subsequently with Podocalyxin.

(A-B'') Crb2a immunostaining in *Tg(-0.2myl7:EGFP-podxl)* hearts at 50 (A-A'') and 79 (B-B'') hpf. At 50 hpf, Crb2a localizes to the junctions between CMs at the apical side, coinciding with ZO-1 immunostaining (A'-A'', arrowheads). At 79 hpf, some compact layer CMs are undergoing apical constriction (B, yellow arrowheads), and Crb2a accumulates at these constricting apical membranes, coinciding with Podocalyxin localization (B'-B'', yellow arrowheads). Moreover, Crb2a expression extends to the apical membrane of compact layer CMs co-localizing with Podocalyxin (B'-B'', white arrowheads). At 79 hpf, Crb2a expression was not observed in delaminated CMs (B'-B'', Ø). V, ventricle. Scale bars, 20 μ m.

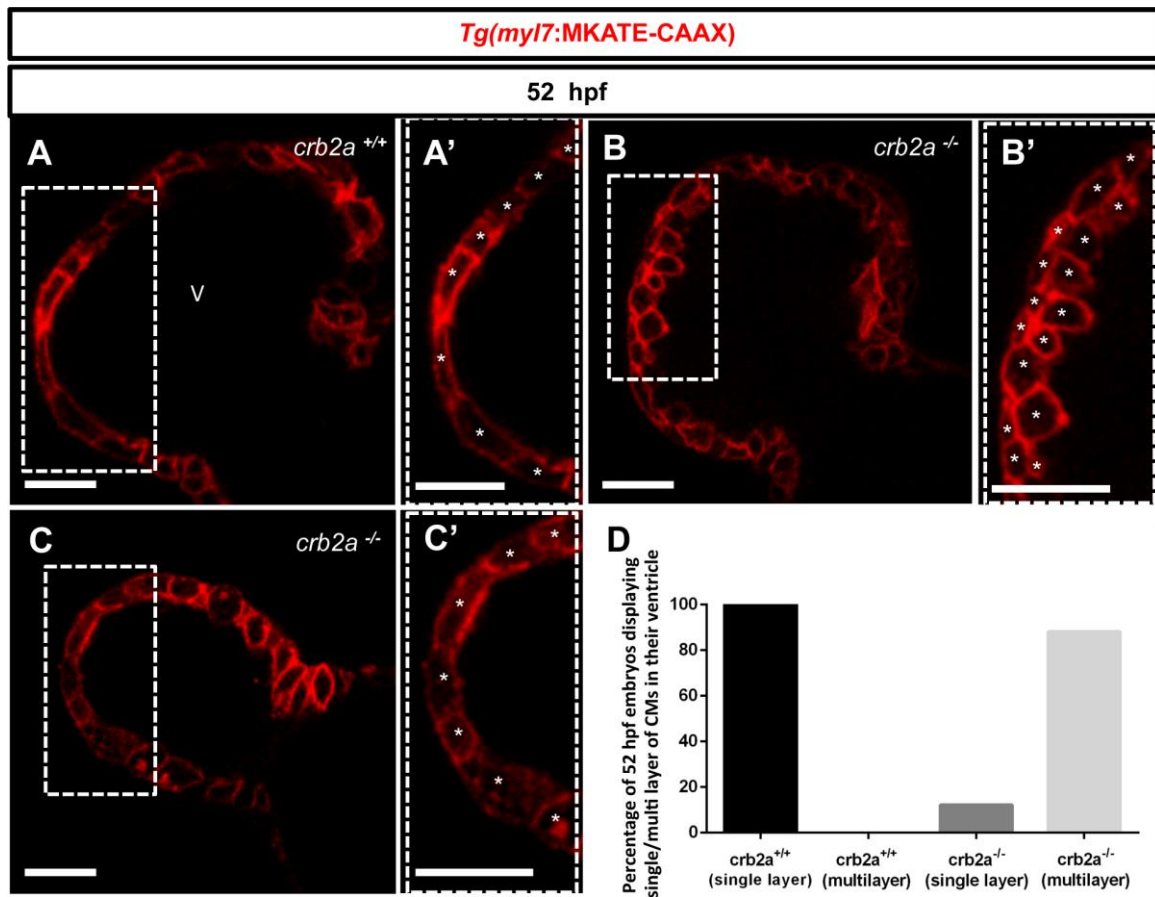


Figure S3. *crb2a*^{-/-} hearts display CM multilayering at 52 hpf

(A-C') Confocal images (mid-sagittal sections) of 52 hpf *Tg(myI7:MKATE-CAAX)* *crb2a*^{+/+} (A-A', n=8) and *crb2a*^{-/-} (B-C', n=22) hearts. Higher magnification images of *crb2a*^{+/+} hearts show a single layer of CMs in the ventricle (A', asterisks). Higher magnification images show a single layer of CMs in the ventricle of 3/22 mutants analyzed (B', asterisks), while the other 19 display multiple layers of CMs in their ventricle (C', asterisks). (D) Percentage of 52 hpf embryos showing single or multiple CM layers in their ventricle. V, ventricle. Scale bars, 20 μ m.

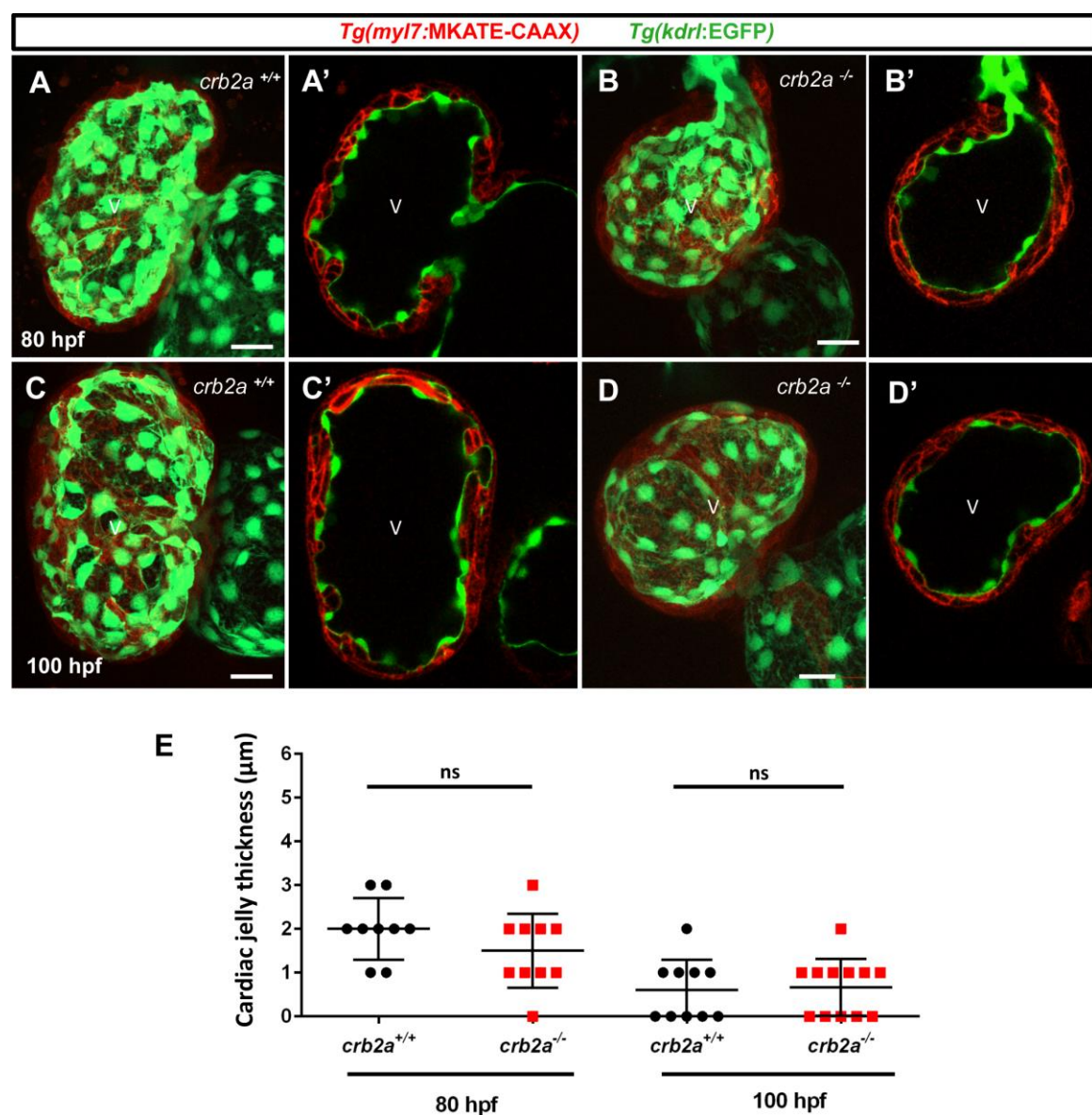


Figure S4. Cardiac jelly reduction is not affected in *crb2a*^{-/-}.

(A-D') Confocal images (maximum intensity projections) of *Tg(kdrl:EGFP)*; *Tg(myI7:MKATE-CAAX)* *crb2a*^{+/+} and *crb2a*^{-/-} hearts at 80 (n=9; n=10) and 100 (n=10; n=12) hpf. *crb2a*^{-/-} hearts display a WT-like reduction of the cardiac jelly at both stages. (E) Quantification of cardiac jelly thickness at 80 and 100 hpf. V, ventricle. Scale bars, 20 μm.

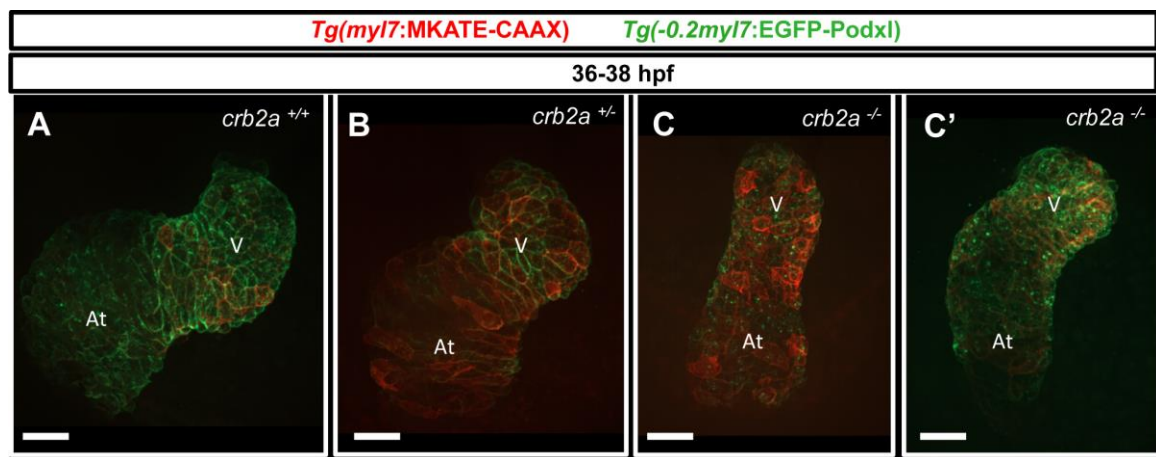


Figure S5. *crb2a* mutant hearts exhibit looping defects.

(A-C') 3D maximum intensity projections of 36-38 hpf *Tg(-0.2myl7:EGFP-podxl)*; *Tg(myl7:MKATE-CAAX)* hearts. Compared to *crb2a*^{+/+} (A (6/6)) and *crb2a*^{+/-} (B (10/11)) hearts, *crb2a*^{-/-} hearts display no looping (C (4/11)) or delayed looping (C' (7/11)). V, ventricle; At, atrium. Scale bars, 20 μm.

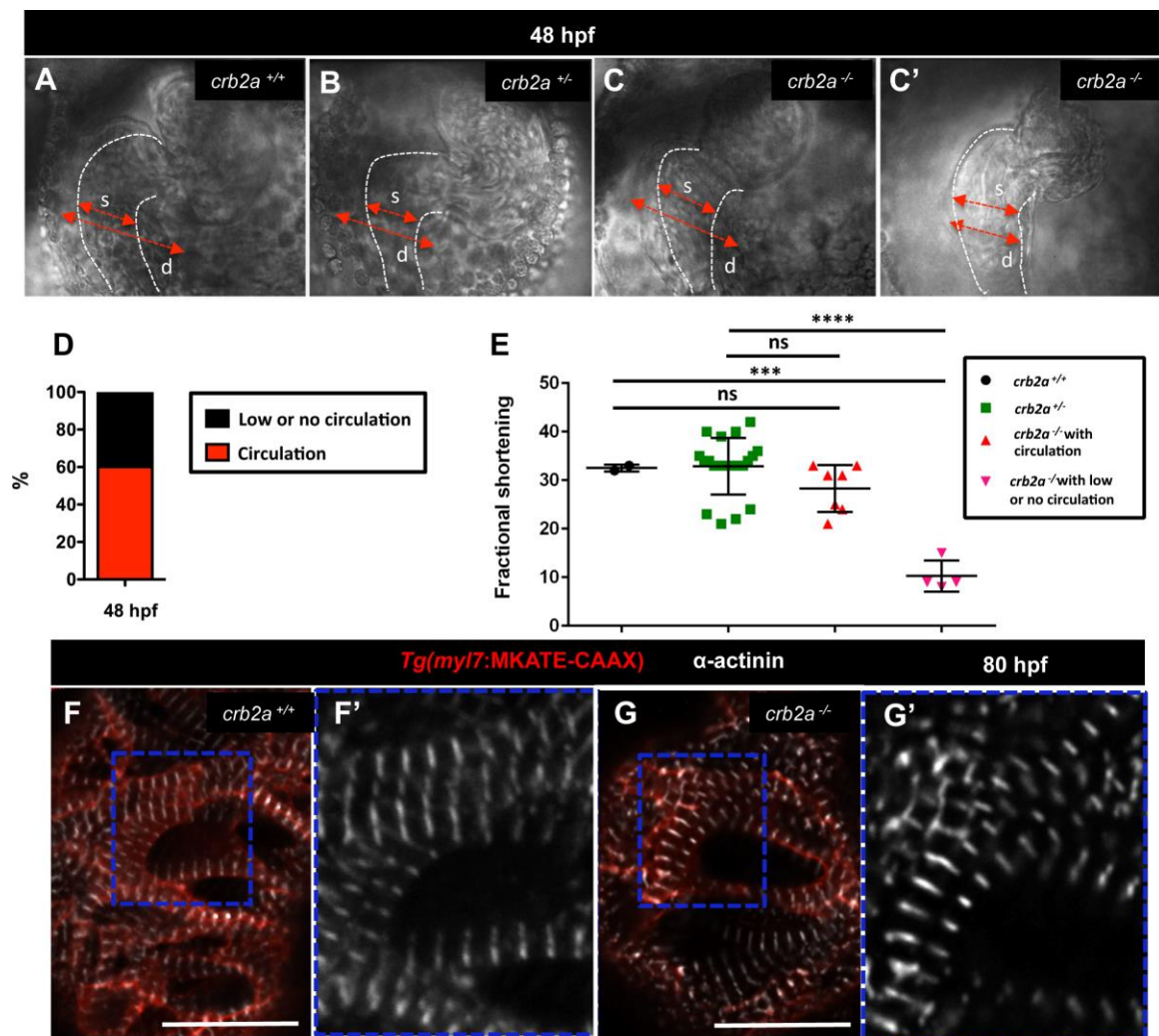


Figure S6. *crb2a*^{-/-} hearts display functional defects at 48 hpf.

(A-C') Brightfield images of 48 hpf hearts. Red arrows indicate length of diastole (d) and systole (s). White dashed lines represent the heart shape in systole. (D) Percentage of mutant embryos with normal, low, or no circulation at 48 hpf. Total number of embryos analyzed: 650; total number of mutants analyzed, 124 (with circulation (n=50), with low or no circulation (n=74)). (E) Fractional shortening of *crb2a*^{+/+}, *crb2a*^{+/-} and *crb2a*^{-/-} hearts. One way analysis of variance (ANOVA) was performed corrected by Tukey's multiple comparisons test; $P < 0.001$, **** $P < 0.0001$. (F-G') Confocal images of α -actinin immunostaining in 80 hpf *Tg(myI7:MKATE-CAAX)* ventricles. Blue boxes show high magnification images of *crb2a*^{+/+} (F') and *crb2a*^{-/-} (G') hearts. Scale bars, 20 μ m.

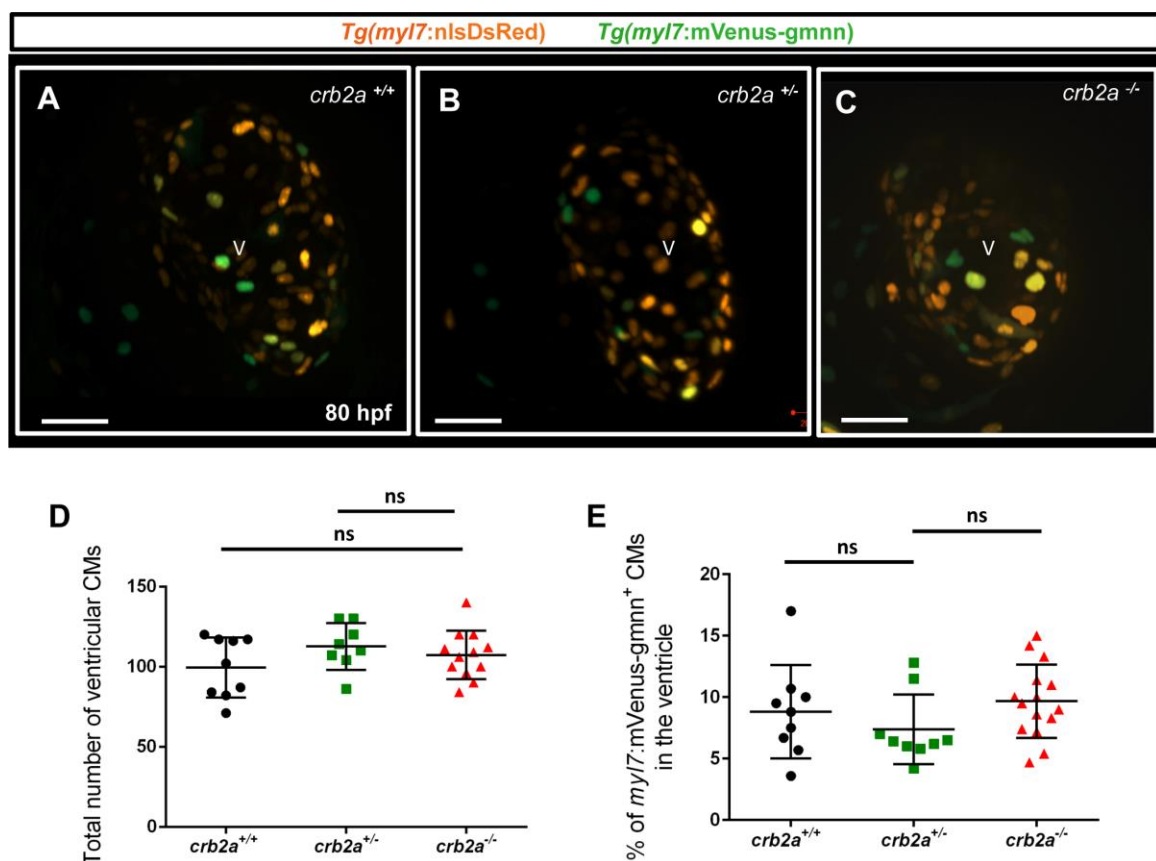


Figure S7. *crb2a*^{-/-} ventricles do not exhibit an increase in CM proliferation.

(A-C) Confocal images (maximum intensity projections) of 80 hpf *Tg(myl7:nlsDsRed)*; *Tg(myl7:mVenus-gmnn)* hearts. (D) Total number of ventricular CMs. (E) Percentage of *myl7:mVenus-Gmnn*⁺ CMs in the ventricle. Each dot represents a heart. One way analysis of variance (ANOVA) was performed corrected by Tukey's multiple comparisons test; ns, no significant differences. V, ventricle. Scale bars, 20 μm.

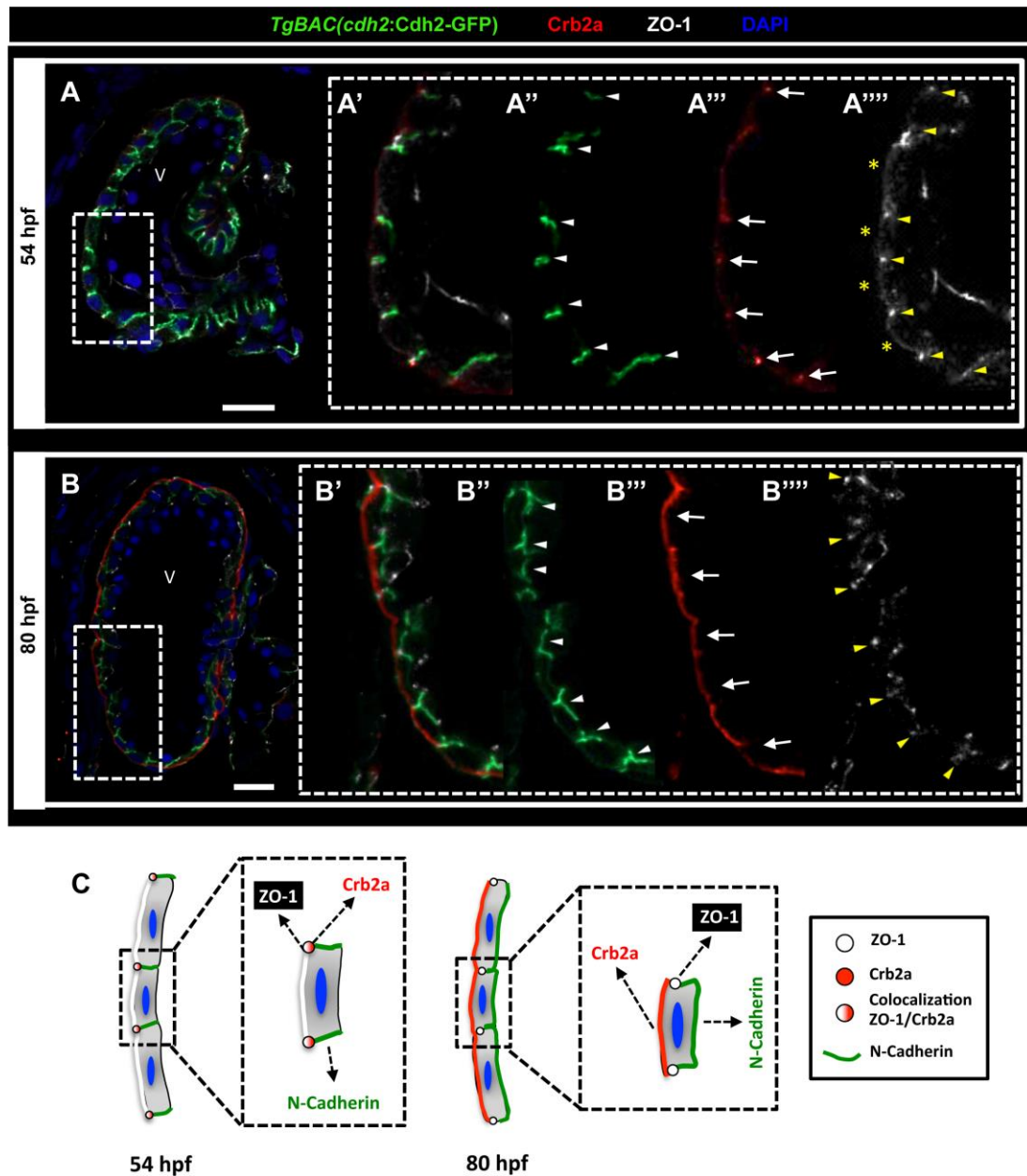


Figure S8. Localization of TJ and AJ proteins and Crb2a in CMs during trabeculation.

(A-B''') Crb2a and ZO-1 immunostainings in *TgBAC(cdh2:Cdh2-GFP)* hearts at 54 (A-A''') and 80 (B-B''') hpf. At 54 hpf, white arrowheads point to lateral localization of N-Cadherin (A''), white arrows point to junctional localization of Crb2a (A'''), and yellow arrowheads and asterisks indicate junctional and apical ZO-1 immunostaining, respectively (A'''). At 80 hpf, white arrowheads point to basolateral localization of N-Cadherin (B''), white arrows point to apical Crb2a localization (B'''), and yellow arrowheads point to junctional ZO-1 immunostaining (B'''). (C) Schematic representation of TJ and AJ proteins in WT CMs. V, ventricle. Scale bars, 20 μ m.

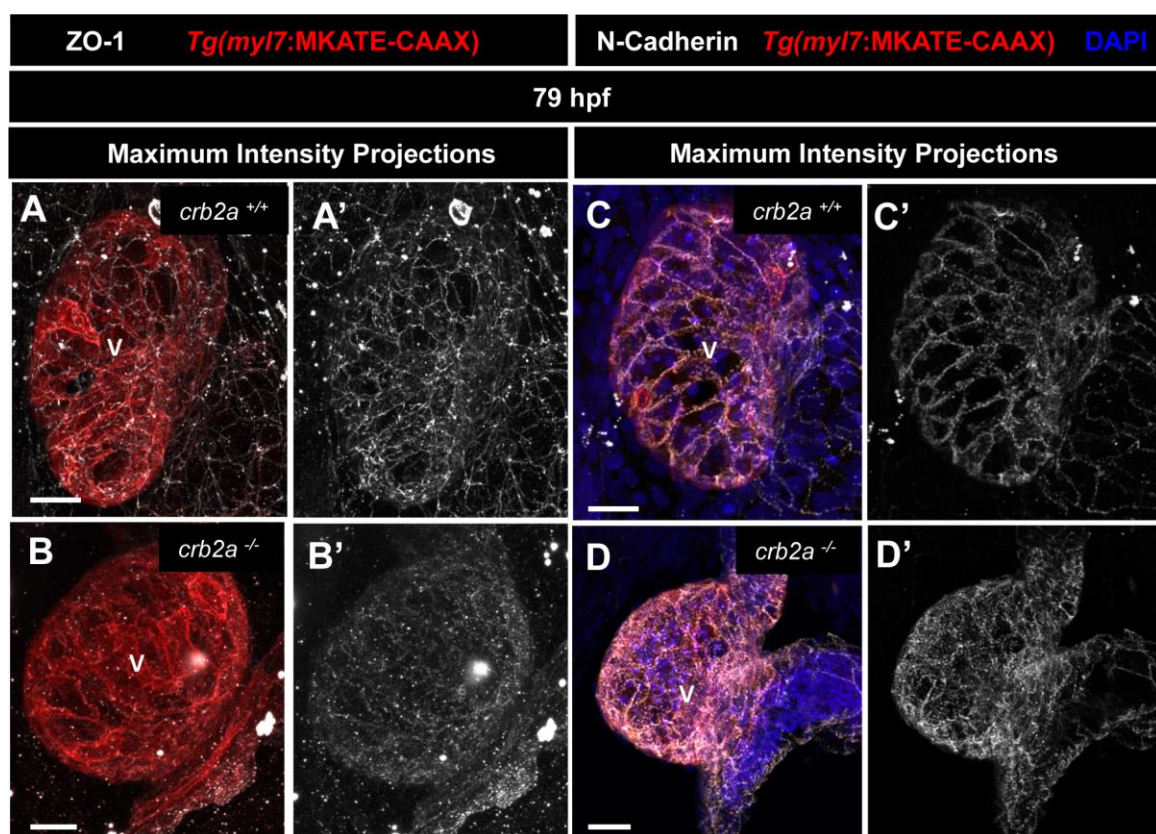


Figure S9. Maximum intensity projection images of TJ and AJ proteins in CMs.

(A-B') Maximum intensity projection images of ZO-1 immunostaining in 79 hpf

Tg(myI7:MKATE-CAAX) hearts show that ZO-1 localizes to the junctions between CMs in *crb2a*^{+/+} (A', n=10), but that its junctional pattern is fragmented in *crb2a*^{-/-} (B', n=16).

(C-D') Maximum intensity projection images of N-cadherin immunostaining in 79 hpf

Tg(myI7:MKATE-CAAX) hearts show that N-Cadherin localizes to the junctions between CMs in *crb2a*^{+/+} embryos (C', n=7), but that it is mislocalized in *crb2a*^{-/-} (D', n=15). V, ventricle. Scale bars, 20 μ m.

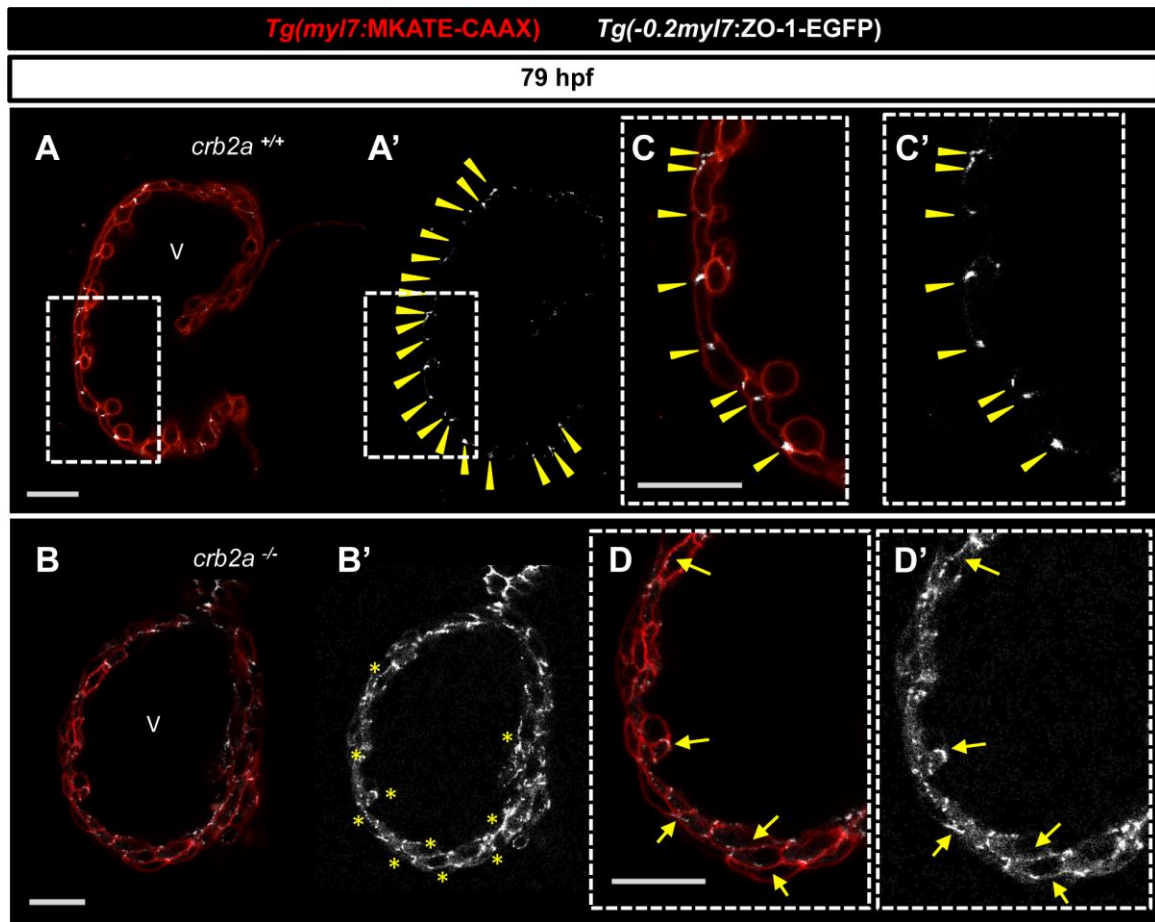
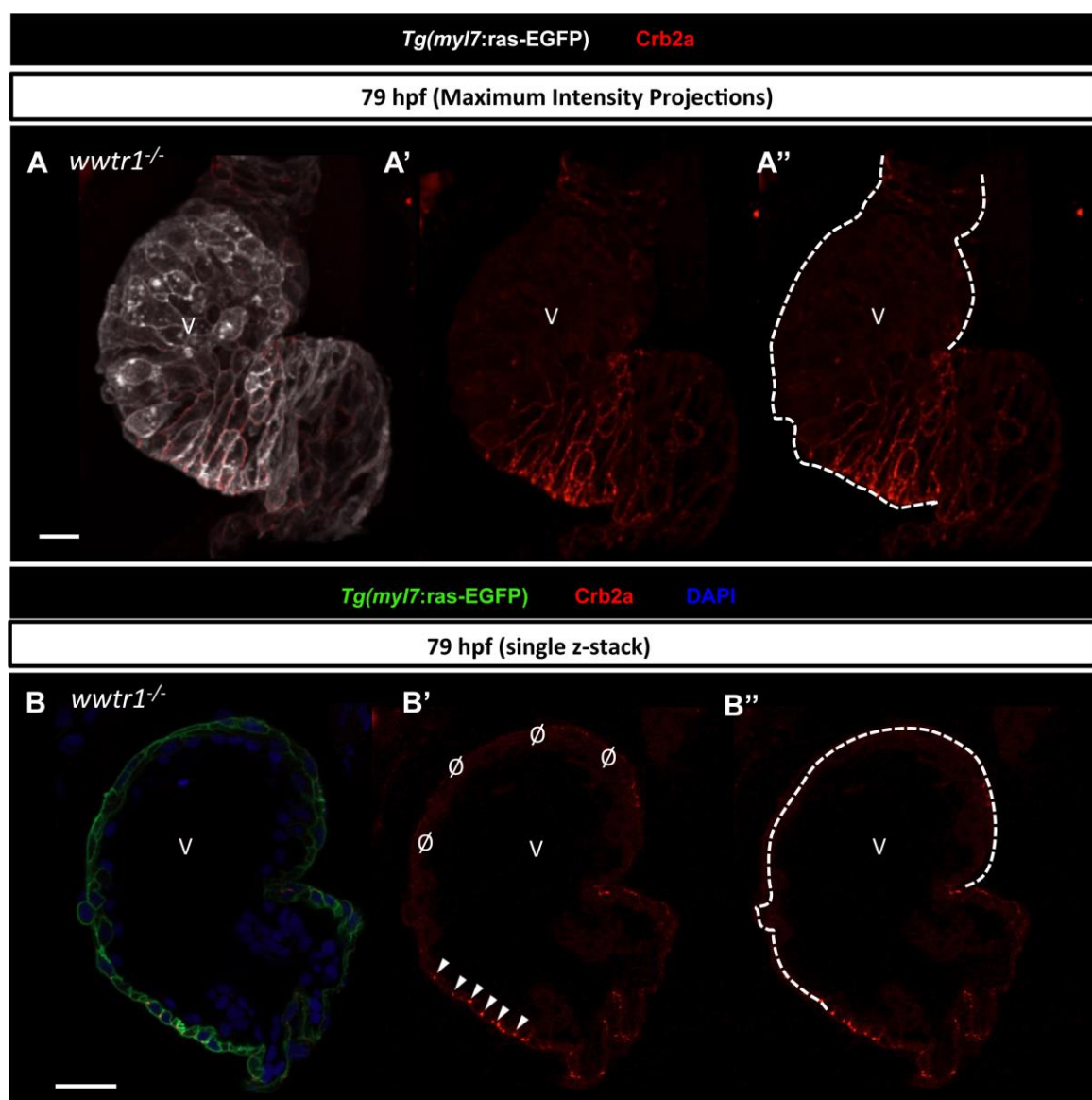


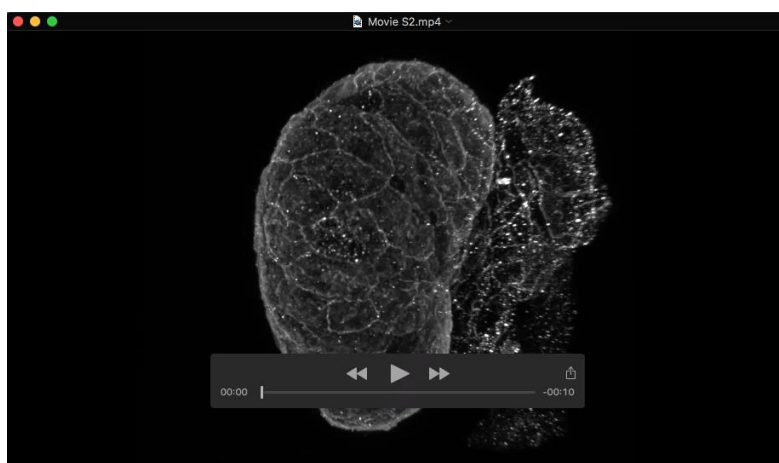
Figure S10. In vivo ZO-1 localization in CMs.

(A-B') Confocal images (mid-sagittal sections) of 79 hpf *Tg(myI7:MKATE-CAAX); Tg(-0.2myI7:ZO-1-EGFP)* *crb2a*^{+/+} (A-A') and *crb2a*^{-/-} (B-B') hearts; higher magnification images (C-D') show that ZO-1 is present at the junctions between compact layer CMs in *crb2a*^{+/+} (A-A' and C-C', arrowheads, n= 12), and that it is mislocalized in *crb2a*^{-/-} (B-B' and D-D', arrows, n=11). V, ventricle. Scale bars, 20 μm.





Movie 1. Movie showing Crb2a immunostaining in 3D reconstructed 51 hpf heart.



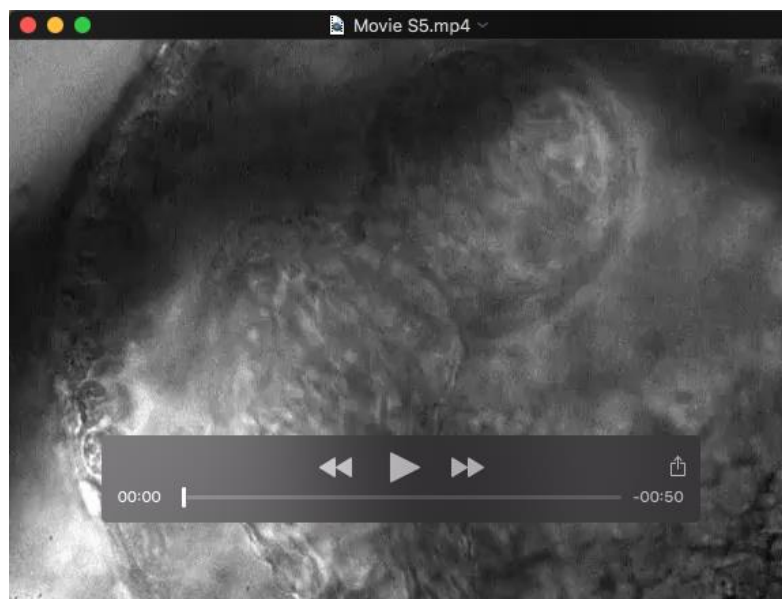
Movie 2. Movie showing Crb2a immunostaining in 3D reconstructed 72 hpf heart.



Movie 3. Movie showing beating of 48 hpf *crb2a*^{+/+} zebrafish heart.



Movie 4. Movie showing beating of 48 hpf *crb2a*^{+/-} zebrafish heart.



Movie 5. Movie showing beating of 48 hpf *crb2a*^{-/-} zebrafish heart with normal circulation.



Movie 6. Movie showing beating of 48 hpf *crb2a*^{-/-} zebrafish heart with low or no circulation.